`

Analysis of Tunneling Current in Heterojunction with Intrinsic Thin Layer (HIT) Solar Cells

By

Amreen Akhtar: 2009-1-80-026
Shuaib Rahman: 2009-2-80-069

Submitted to the

Department of Electrical and Electronic Engineering
Faculty of Sciences and Engineering
East West University

in partial fulfillment of the requirements for the degree of
Bachelor of Science in Electrical and Electronic Engineering
(B.Sc. in EEE)

Fall, 2012

Approved By

_____	_____
Thesis Advisor	Chairperson
Dr. Anisul Haque	Dr. Mohammad Mojammel Al Hakim

`

Authorization page

We hereby declare that we are the sole authors of this thesis. We authorize East West University to lend this thesis to other institutions or individuals for the purpose of scholarly research.

_____

Amreen Akhtar

_____

Shuaib Rahman

We further authorize East West University to reproduce this thesis by photocopy or other means, in total or in part, at the request of other institutions or individuals for the purpose of scholarly research.

_____

Amreen Akhtar

_____

Shuaib Rahman

`

Abstract

Heterojunction solar cells have proved to exceed the efficiency barrier that homojunction solar cells have tried to cross for decades. Among the most efficient heterojunction solar cell structures, the Heterojunction with Intrinsic Thin Layer or HIT is the most popular. The simplest form of HIT structure is: Amorphous P-type Semiconductor/Intrinsic Semiconductor/Crystalline N-type semiconductor, or vice versa.

In a heterojunction, due to the difference in bandgap of the materials, a potential barrier forms that creates obstacle for the electrons/holes to travel from one side to the other. Such trapping of electrons/holes reduces the efficiency of the solar cell. However, a fraction of these electrons/holes pass the potential barrier through Quantum Tunneling and create a tunneling current, which contributes to the overall current; hence improving the efficiency.

In this document, the tunneling current of a P-type a-Si/I-Si/N-type c-Si HIT structure is studied. The length of the P-type amorphous layer, intrinsic layer and the N-type crystalline layer is varied to study how the thickness of each layer impacts the tunneling current. Also, the impact of doping densities of the P-side and N-side on the tunneling current is analyzed. Varying these parameters (thickness and doping) an optimized combination of a simple HIT structure is proposed for which the tunneling current is maximum.

By analyzing the effects of thickness and doping densities, it is seen that the maximum tunneling current is observed for5 nm P-side thickness and 4 nm intrinsic thickness; with doping density $10^{19}cm^{-3}$ at P-side and 10^{13} cm^{-3} at N-side.

`

Acknowledgements

Sincere gratitude to our honorable supervisor Dr. Anisul Haque, Professor, Department of Electrical and Electronic Engineering, for his kind guidance and constant effort to make us work forperfection. His patience and immense knowledge has been of a constant source of motivation. Special thanks to the Chairperson of the department, Dr. Mohammad Mojammel Al Hakim, for every cooperation and support.

We would also like to thank our honorable teachers, who have worked effortlessly to develop our understanding on subject matters throughout the process. It is because of their constant endeavorsthat we have grown with every passing day, a small step at a time.

We are grateful to everyone who have helped us directly and indirectly with information, motivation and support. We are grateful indeed.

May Allah, the Merciful, bless and guide us all.

`

TABLE OF CONTENTS

`

LIST OF ILLUSTRATIONS

LIST OF TABLES

`

Chapter 1: Introduction

1.1 Background

Heterojunction devices are playing an increasingly important role in optoelectronics. These are produced combining semiconductors that have differing bandgap energies. Scientists in the late 1950s discovered the possibility of using two different semiconductors to form a heterojunction,unlike a homojunction. The early 1970s brought about increased interest in heterojunction for various areas of devices applications. In fact, the production of a room-temperature heterostructure laser demonstrated the feasibility of a new generation of devices whose performance would have been impossible with the conventional homojunction devices[1].

After the first solar cell made up of silicon was demonstrated 55 years ago [2], the cost has declined by a factor of nearly 200. The fantastic boom of thin film technology in recent years suggests further development on the solar cell due to the application of innovative concepts to conventional materials and developments.New classes of thin film materials are stemming from nanotechnologies, photonics, and new semiconducting organic and inorganic sciences.

In the last decade Sanyo has successfully commercialized the Heterojunction with Intrinsic Thin Layer solar cell (HIT), which consists of a doped hydrogenated amorphous silicon (a-Si:H) layer and a thin intrinsic amorphous silicon layer on top of a crystalline silicon (c-Si) absorber.

The HIT solar cell has many advantages over the silicon homojunction solar cell, such as structural simplicity,high efficiency with no complicated structural techniques, low-temperature process due to the use of amorphous Si layer(< 200°C) and so on. This causesa drastic decrease in price of solar cell [1].

1.2 Literature Review

The idea of silicon based heterojuction solar cells first came from University of Marburg, Germany [1]. However, to obtain a reasonable open circuit voltage, a very thin intrinsic hydrogenated layer needed to be introduced between the P-layer and N-layer; unlike the

`

homojunction solar cells. Increased doping density in a-Si increases the defect density, hence increases the interface defect density of the heterojunction, which results in a lower open circuit voltage[1].Thissubsequently led to successful commercialization of the HIT concept by Sanyo, adding a thin intrinsic semiconductor layer between the P and the N type[1], [3].Later in May 2009 Sanyo formally announced an achievement of 23%efficiency in HIT solar cell, which was later published in 2010[4]. This was achieved through several stages of development in the HIT design, such as introducing textured wafer surfaces for light trapping, adding double sided passivation to the wafer, improvement in the quality of the heterojunction, grid electrodes, and the Thin Conducting Oxide (TCO) and optimization of material and processing.Significant development on use of heterojunction to create high efficiency solar cells can be observed. Many alternative concepts have been developed through the increasing research on this field. The expiration of Sanyo's patent in 2010 has inspired even a larger number of publications and research on heterojunction solar cell over the last few years.

A potential barrier forms in the energy band in case of heterojunctions which acts as an obstacle on the electrons or holes. These trapped electrons/holes either gain energy and jump over the energy barrier, and a fraction of it tunnel through the barrier by a process known as quantum tunneling. The tunneling current adds to the overall current and therefore, has influence on the efficiency. Simulation results suggest that tunneling in the P/N interface and the ITO/p-type interface plays a vital role in carrier transport process [1], [5]. To mention, ITO or Indium Tin Oxide is a popular transparent conducting oxide layer, which is widely used in solar cells as contact. The significance of the role of tunneling current on the overall performance has led to several publications on numerical modeling for integrating tunneling current calculation with the thermionic emission in heterojunction solar cells; that includes tunneling current module for the heterojunction simulation softwares as well [6], [7].

The process of tunneling plays an important role based on the design and operating condition of the device[1]. However, the Sanyo model did not consider the analysis of tunneling current as a separate parameter with changes in the thickness of the layers and doping. High doping on the P-side and low doping in the N-side is considered to give higher efficiency [1].

`

1.3 Objective

The objective of this document is to analyze the tunneling current of a simple N-type HIT structure, made up of P-type amorphous Si layer, intrinsic Si layer embedded in N-type crystalline Si.

In order to calculate the tunneling current, the HIT structure and the potential profile of the deviceis simulated using Afors-Het. Afors-Het is a computer based simulation software that is able to simulate both homojunction and heterojunction solar cells. The simulation data is further used to calculate the transmission coefficient using WKB approximationand hence the tunneling current is calculated.

Furthermore, the thicknesses of the P-layer and the intrinsic layersare varied to observe and determine the optimized thickness combination that gives the highest tunneling current.Similarly, doping density at the P-side and the N-side is varied to determine the optimized doping densities of both sides that give maximum tunneling current.

As a result, a specific combination of thickness and doping densities of HIT structure is obtained that gives the maximum tunneling current with these experimental results.

`

Chapter 2: Hit Solar Cell Structure

2.1 Basic Structure of HIT Solar Cell

Heterojunction solar cells based on amorphous and crystalline silicon are very suitable devices for low cost and high efficiency energy conversion. Sanyo has successfully achieved an efficiency of 23% using heterojunction technology [4]. The a-Si:H/c-Si heterojunction solar cells with a thin intrinsic layer clearly demonstrates its feasibility as a concept for high efficiency solar cells compared to conventional c-Si solar cells.A considerable cost reduction is also achieved as the fabrication process can take place at temperatures below 200^{o}C [8].

In this document the structure of heterojunction (HIT) solar cell discussed is an N-type HIT solar cell, where the absorber is N-doped and the semi-permeable membrane is P-doped. The injection of electrons from the absorber into the P-type semiconductor can be suppressed by use of amorphous P-type semiconductor with a larger bandgap than that of the absorber. The bandgap differences give rise to valence and conduction band discontinuities, respectively, and act as hole or electron reflecting barriers and suppress the undesirable carrier recombination at anode and cathode contacts. The asymmetry between the electronic structure of N-type and P-type semiconductors is the basic requirement for photovoltaic energy conversion.Figure-1 shows the structure of a simple HIT solar cell with the P-type a-Si:H of width 5nm, intrinsic a-Si:H of width 4nm and N-type a-Si:H of width 300um.

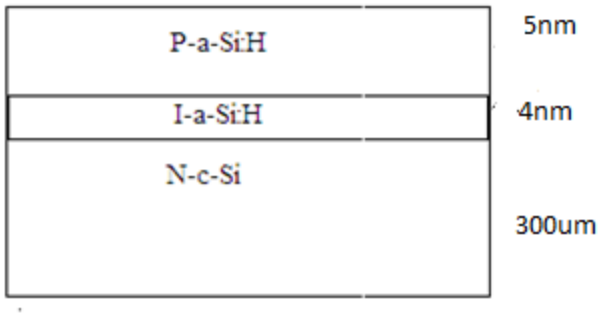

Figure 1: The structural diagram of a HIT solar cell with a-Si:H(P)/I-layer and c-Si(N) layer.

`

Figure-2 shows the energy-band diagram of a simple heterojunction.A thin hydrogenated amorphous silicon (a-Si:H) used as a wide bandgap layer of 1.75 eV, acts as the semi permeable membrane, over crystalline silicon (c-Si) of bandgap 1.1 eV. The minority carrier electrons from the P-type a-Si:H layer can easily go to n-type but a transport barrier is formed for the holes at the interface between the two materials. The holes can pass through narrow 'spike' barriers by either thermionic emission or by quantum tunneling.

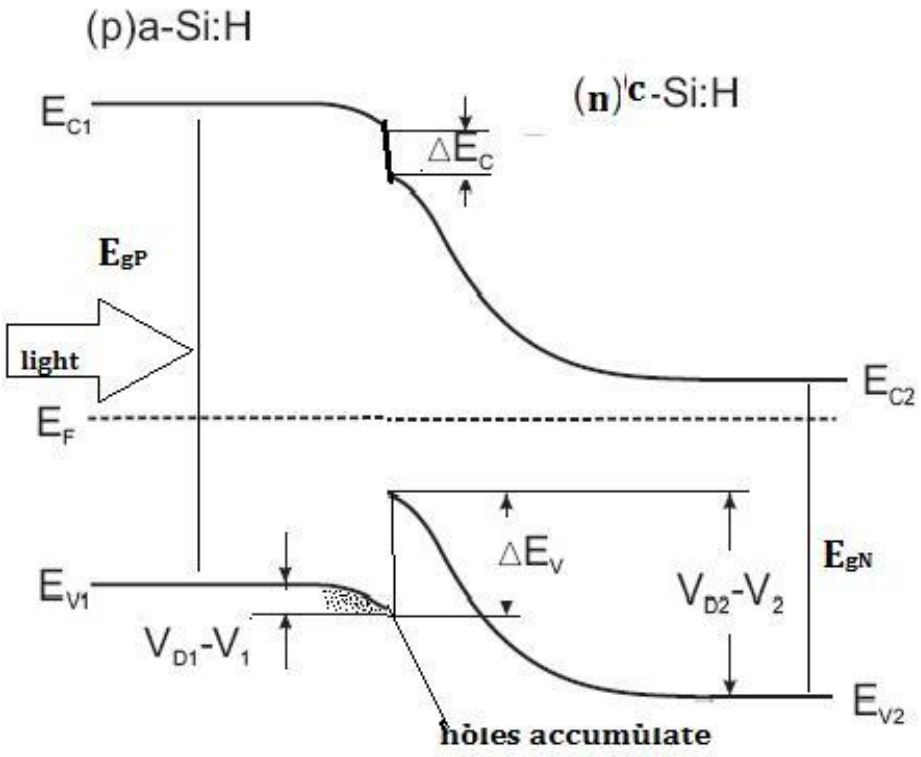

Figure 2: Band diagram of an a-Si/c-Si heterojunction.

In summary, in a heterojunction solar cell the injection of one type of charge carriers from the absorber into membrane materials, in which they become minority carriers and recombine, can be suppressed. This can result in a more efficient use of photo-generated carriers and consequently a higher photocurrent.

`

2.2 The Importance of Amorphous Layers in HIT Structure

The design of the silicon heterojunction solar cell are produced by low temperature growth of ultra-thinlayers of amorphous silicon (a-Si:H) on both sides of a thin crystalline siliconwafer-base, less than 200 µm in thickness, where electrons and holes are photo-generated [1].

The a-Si:H/c-Si heterojunction solar cell is a good solution to the problems associated with high-temperature junction formation because a-Si:H can be deposited at temperatures below 200º C [8]. The HIT solar cell features excellent surface passivation due to the amorphous Si layer (a-Si:H), and so has a higher V_{oc}than the homojunction solar cell. However, the incorporation of a-Si:H layers in HIT solar cells causes light absorption losses, which result in a lower J_{sc}. Hence the a-Si:H layers in heterojunction silicon solar cells are very thin (only several nanometers) and provide a negligible contribution to the overall power generation. Effective a-Si:H/c-Si interfaces that allow efficient transport of charge carriers with minimal recombination loss is a prerequisite for high-performance heterojunction solar cells. The graphs of V_{oc} ,J_{sc}, FF (in fraction) and Efficiency (in fraction) below shows the change in the P-type Si width from 1 nm to 40 nm, with the fixed intrinsic layer of 4 nm:

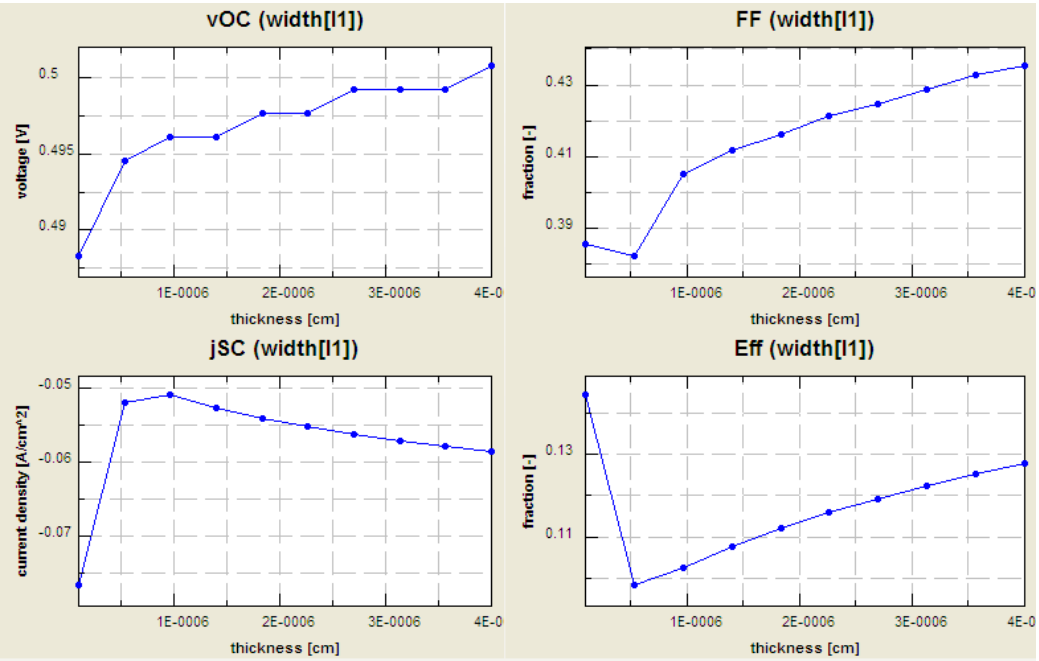

Figure 3 : The impact of changing length of P-type a-Si thickness on various parameters, with intrinsic a-Si 4 nm.

`

Advantages of using the a-Si:H layer are:

1. Solar cell with improved surface passivation, and a correspondingly higher V_{oc}.
2. Improved temperature dependence.

2.3 Electronic Transport across the HIT Solar Cell

In a n-type HIT solar cell, at dark condition a forward bias voltage is givendue to which a small fraction of band bending in the a-Si:H, shown in Figure-2, will reduce the band bending in the c-Si [9]. It is easily seen thatwhen a moderate forward bias V is applied, the electrons coming from the c-Si have to pass a barrier of $(V_{D1} - V_1) + (V_{D2} - V_2) + \Delta E_C$. The holes coming from thea-Si:H side on the other hand have to surpass $(V_{D1} - V_1) + (V_{D2} - V_2) - \Delta E_V$unless the fraction of the voltage drop supported in c-Si is less than $\Delta E_V$with increasing V,which is $(V_{D2} - V_2) \geq \Delta E_V$. When both carriers are considered, the equation of the current across the junction is denoted in equation (1). The first term of the equation describes the contribution of holes crossing the junction from the amorphous side, while the second term is the electrons originating from the c-Si of the junction. If $V_{D2} - V_2 < \Delta E_V$applies, the contribution of the holes to the current changes. Instead, the hole current across the junction is expressed as shown in equation (2).

$$j_F = \left[\frac{eD_{p,c-Si}}{L_{p,c-Si}} N_{A,a-Si:H} T_h \exp\left(-\frac{q\Psi_{bi} - \Delta E_v}{kT}\right) + \frac{eD_{n,a-Si:H}}{L_{n,a-Si:H}} N_{D,c-Si} T_e \exp\left(-\frac{q\Psi_{bi} + \Delta E_c}{kT}\right)\right]\left[\exp\left(\frac{qV}{kT}\right) - 1\right] \quad (1)$$

The hole current equation is expressed as,

$$j_{hole} = \frac{eD_{p,c-Si}}{L_{p,c-Si}} N_{A,a-Si:H} T_h \exp\left(-\frac{q\Psi_{bi}}{(1+a)kT}\right) \times \left[\exp\left(\frac{qV}{(1+a)kT}\right) - \exp\left(-\frac{aqV}{(1+a)kT}\right)\right] \quad (2)$$

Where,

$$a = \frac{V_{D1} - V_1}{V_{D2} - V_2} \quad (3)$$

Here,

`

$N_{\frac{D}{A}}$ is the donor/acceptor concentration, $D_{\frac{p}{n}}$ is the diffusion constant, $L_{\frac{p}{n}}$ is the diffusion length in respective materials, $\Psi_{bi} = V_{D1} + V_{D2}$ is the built in voltage, $V = V_1 + V_2$ is the partition of externally applied voltage, ΔE_c and ΔE_v are the conduction and valence band and T_e and T_h are transmission coefficients of electrons and holes respectively, *a* is the ratio of the voltagedrops supported by the two materials.This expresses the fraction of carriers that overcomes the barrier represented by band offsets.

At light condition, the standard solar spectrum ofAM 1.5 is incident on the HIT solar cell. The P-type Si has higher band-gap so that all high-energy photons that have energy greater than bandgap of P-type (E_{gP}) are absorbed. Similarly the low-energy photons that have energy lower than bandgap of N-type (E_{gN}) are absorbed by the N-type c-Si.

Once the electron-hole pairs are formed in the layer, the carriers from both parts flow in the direction directed by the field and the gradient of charge carriers, by drift and diffusion respectively. The transport of electrons inside the bulk c-N-Si, is dominated by diffusion. However, it is well known that tunneling does not play an important role in conventional semiconductor/metal structures at room temperature, especially for high barriers and/or low doping levels. The dominant mechanism for current injection in this case is thermal emission [10].

In this document the tunneling current is analyzed at low reverse bias where the diffusion current is minimum. The ultra thin P-type is a-Si of 5 nm with heavy doping (10^{19} cm^{-3}), whereas the N-type absorber is c-Si which is of 300 um and nominally doped (10^{14} cm^{-3}). The difference in the doping and the band-gap of amorphous silicon and the crystalline silicon creates a barrier at the valance band, which will trap the holes moving from the P-side to N-side,thus rendering alternative transport paths of tunneling into the transport system [10].

`

Chapter 3: Quantum Mechanical Tunneling in Heterojunctions

Tunneling of particles through potential barriers is a phenomenon that cannot be explained through classical physics. Any particle can be represented as a wave function in quantum physics. At the wall of the finite potential barrier, the wave function does not terminate, rather it can penetrate into and through the barrier. Thus, the probability of a particle tunneling through a barrier of finite height and width is not zero [11]. The tunneling of such particles is known as quantum tunneling.

The current that can be found from tunneling of holes and electrons is known as tunneling current. Many modern world electronic devices, like tunnel diode, scanning tunneling microscopes and TFETs (Tunnel Field Effect Transistors), are designed based on quantum tunneling principle.

3.1 The Importance of Hole Tunneling in N-type HIT Solar Cell

Heterojunction is a junction between materials of different bandgaps (E_g). The difference in bandgap creates a band offset in the energy-band diagram, discussed in Chapter 2, Section 2.1. A N-type HIT solar cell uses a N-type c-Si bulk and a-Si to form a heterojunction, which creates a band offset. This can be understood using Anderson's rule, also known as Electron Affinity Rule. The equations to express the band offsets at conduction band and valence band respectively are as follows [12].

$$\Delta E_C = \chi_B - \chi_A \quad (4)$$

$$\Delta Ev = (\chi_A + E_{gA}) - (\chi_B + E_{gB}) \quad (5)$$

Where,

`

χ_A and χ_B are electron affinities of materials A and B respectively, $E_{gA}$and E_{gB} are bandgaps of materials A and B respectively andΔE_c and $\Delta E_v$are the band offsets of conduction band and valence band respectively.

Figure-4 shows the isolated P-type and N-type Si and their band energies.

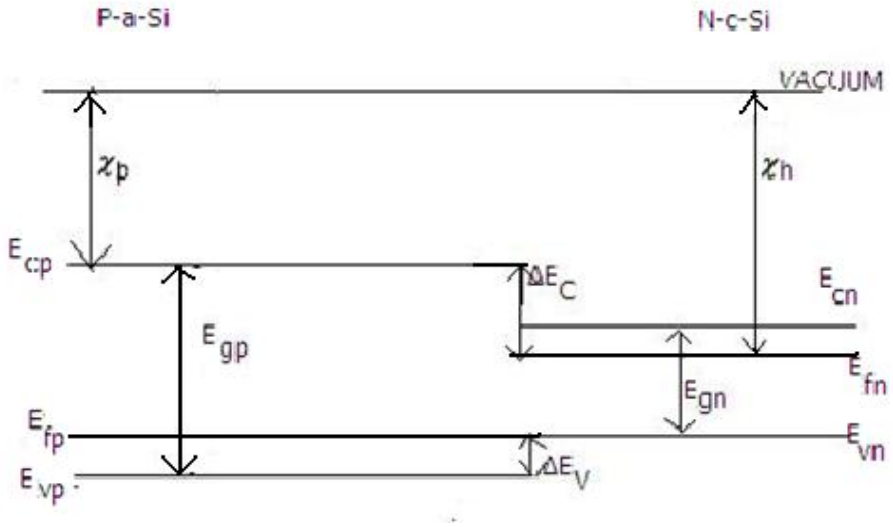

Figure 4: Energy-Band diagram of isolated P-type a-Si and N-type c-Si.

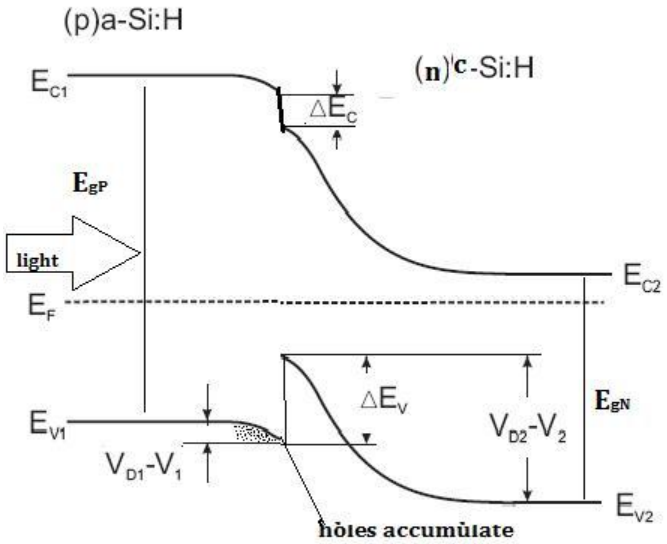

Figure 5: Schematic equilibrium energy-band diagram of the P/N heterojunction between P-type a-Si and N-type c-Si.

`

In a N-type HIT structure, a potential barrier forms at the valence band due to bandgap difference of a-Si and c-Si, which traps holes from the incident side (as can be seen in Figure 5) . Such trapping of holes creates an obstacle for hole transportation and thus reduces the overall current. But due to quantum tunneling, a fraction of the trapped holes tunnel through the potential barrier and contribute to the overall current. With heterojunctions, current due to this tunneling can be significant.Simulation results show that tunneling plays a vital role in carrier transport through the P/N heterojunction interface, hence inheterojunction solar cells based on N-type c-Si wafers[1], [5].

3.2 Transmission Coefficient and Tunneling Current

In quantum mechanics, Transmission Coefficient and Reflection coefficient together describe the behavior of a wave on an incident barrier. The transmission coefficient is the measure or probability of the incident wave tunneling to the other side of a barrier relative to the reflected wave; derived from the solution of the wave functions. Together, they add up to a probability of 1.

In case where the potential barrier does not vary rapidly, Wentzel-Kramers-Brillouin approximation or WKB approximation is the most commonly used method to calculate the transmission coefficient, especially when the shape of the potential barrier makes it complicated to calculate the transmission coefficient [11]. Using one dimensional WKB approximation, the transmission coefficient as a function of energy, is expressed as shown in equation (6) [11]:

$$T(E) \approx \exp\left[-2/\hbar \int_{x1}^{x2} \sqrt{2m^*[V(x) - E]}\, dx\right] \qquad (6)$$

Where,

$\hbar$ = h/2π, h being the Plank's constant, m* is effective mass, *x1* and *x2* are the classical tunneling points, E is the energy of the incident wave function and$V(x)$is the potential profile as a function of distance.

Tunneling current is the current due to the tunneling of particles through potential barriers. In nano scale low temperature operation and high doping density, the tunneling current becomes more

`

significant [11]. It is proportional to the transmission coefficient, and dependent on density of states on both sides of the potential barrier, and probability of occupation derived from the Fermi-Dirac distribution on both sides [11]. The equation of tunneling current density can be expressed in several simplified forms based on the device design. The tunneling current density across a potential barrier can be found from the following equation [13].

$$J = \frac{e}{2}\int_{E_1}^{E_2} |T(E)|^2\, n(L,E)\, v(L,E)\, dE - \frac{e}{2}\int_{E_1}^{E_2} |T(E)|^2\, n(R,E)\, v(R,E)\, dE \tag{7}$$

With,

$$v(R,E) \textbf{ and } v(L,E) = \frac{\hbar}{m^*}k \tag{8}$$

and $$k = \sqrt{\frac{2m^*(E - E_v)}{\hbar^2}} \tag{9}$$

Here,

e is the charge of electron, $n(L,E)$ is the number of electrons/holes as a function of position and energyon the left side of the barrier, $n(R,E)$is the number of electrons/holes, as a function of position and energy on the right side of the barrier, $v(L,E)$ is the velocity of electrons/holesas a function of position and energy on the left side of the barrier, $v(R,E)$ is the velocity of electrons/holes as a function of position and energy on the right side of the barrier, $E_v$is the valence band energy and $E_1$and $E_2$are theenergy limits over which the tunneling current is calculated.

`

Chapter 4: Simulation Using Afors-Het

The energy-band diagrams for several length combinations of P-Si and I-Si, with changed doping densities of P-side and N-side are simulated using Afors-Het 2.4. The data from the energy-band diagram is further used to calculate transmission coefficient and tunneling current at the potential barrier of the valence band.

4.1 Introduction to Afors-Het

Afors-Het is an on demand open source 1D/2Dcomputer simulation program for heterojunction devices, which is able to handle homojunctions as well[1].It is widely used for simulation purpose of solar cells. The program allows for arbitrary parameter variations in order to match simulated measurements to real measurements. It is developed by Helmholtz-Zentrum, Berlin. Helmholtz-Zentrum is a research body, specialized on heterojunction researches.

Afors-Het is able to deal with multiple stacks of different semiconductor layers. The following provisions are included into the simulation module for calculation[1].

i. Inclusion of the interface defects that enables it to calculate both bulk recombination and interface recombination.
ii. Interface models(drift/diffusion and thermionic) based on electron/hole transportation across heterojunction interface.

`

iii. The semiconductor material properties of the layers, i.e. linear, exponential, Gaussian etc.

iv. The front and back contact of the device can be modeled as Schottkyboundary, insulator boundary or metal/insulator/semiconductor boundary for diverse experimental configurations.

v. Multidimensional parameter variation.

A detailed discussion on all implemented models in Afors-Het can be found in[14].

Afors-Het simulation calculation module is subdivided into 2 steps: optical simulation and electrical simulation.

4.1.1 Optical Simulation

For electron and hole generation rate due to photon absorption, two categories of generation, namely super bandgap generation (energy of the photon ≥ bandgap) and sub bandgap generation (energy of the photon ≤ bandgap), is made. The sub bandgap generation is calculated in the electrical modeling part, as it is dependent on local particle densities. The optical super bandgap generation is equal for electrons and holes.

So far, two optical models are included. They are Lambert-Beer optical absorption model and optical model for coherent/incoherent internal multiple reflections. The Lambert-Beer model is specially suited to treat c-Si wafer based solar cells. The second model takes coherence effects into account, but is done only for plain surfaces.

Lambert-Beer model allows multiple forward and backward traveling of light to be taken into consideration, but does not take coherence interference into account. Both constant and changing values of absorbance and reflectance can be used for calculations. The angle by which the incident light travels through the layer stack is dependent on the wavelength of the incident light. It is calculated using Snelliu's law, using the following equation[1]:

$$\gamma(\lambda) = \delta - arcsin\left(\frac{\sin(\delta)\ 1}{n(\lambda)}\right) \qquad (10)$$

`

Here,

$\gamma(\lambda)$ is the angle of the incident light passing through the layer, δ = 54.7° for textured silicon wafer with <111> pyramids whereas δ = 0° for normal incidence, λ is the wavelength of the incident light and $n(\lambda)$ is the refraction index for the first layer semiconductor at the illuminated side (function of the wavelength).

It is assumed that all photons of specified wavelength cross the layer stack under distinct angle γ. Photon absorption is then calculated from the spectral absorption coefficientof the semiconductor layer corresponding to the position of the stack, expressed as

$$\alpha_x(\lambda) = {4\pi k(\lambda)}/{\lambda} \qquad (11)$$

Where,

$k(\lambda)$ is the extinction coefficient. The super bandgap electron-hole generation rate for a standard solar spectrum (AM 1.5) incident on the semiconductor layer for single run through is given by:

$$G(x,t) = \int_{\lambda_{min}}^{\lambda_{max}} d\lambda . \phi(\lambda,t) . R(\lambda) . A(\lambda) . \alpha_x(\lambda) e^{\frac{-\alpha_x(\lambda)x}{\cos(\gamma)}} \qquad (12)$$

Here,

λ_{max} and λ_{min} are maximum and minimum wavelength of the incident light respectively, $\phi(\lambda,t)$ is the incoming spectral photon flux and $R(\lambda)$ **and** $A(\lambda)$ are reflectance and absorbance respectively.

Hence, if coherence effects can be neglected, the optical generation rate can be calculated as,

$$G(x,t) = G_n(x,t) = G_p(x,t) \qquad (13)$$

4.1.2 Electrical Simulation

`

For all the arbitrarysemiconductor layers, Poisson's equation and continuity equation for electrons and holes need to be solved to perform the calculations for electrical simulation. Different physical models are used to describe current in each semiconductor/semiconductor interface and front and backside boundaries. This leads to a system of non linear three dimensional differential equations with respect to time and space derivatives. The system of differential equations is solved for the independent variables, i.e. electron density, hole density and electric potential.

The Poisson's equation is expressed as:

$$\nabla^2 \phi = -\frac{\rho}{\epsilon} \tag{14}$$

Here,

ϵ is the electric permittivity of silicon, ϕ is the electric potential across the interface and ρ is the local charge density, which is the sum of all fixed and mobile charges.

Boundary conditions are applied to solve Poisson's equation for electric potential. The boundary condition commonly applied for semiconductor interface is,

$$E(0^-) = E(0^+) \tag{15}$$

Which implies the electric field just before the edge of the interface barrier and electric field just after the edge of the interface barrier are equal, as electric field is a continuous quantity.

In case of DC simulation, the time derivatives are absent, resulting in a simplified system of differential equations. The set of differential equation is then solved for time independent, but position dependent functions. In DC mode, the equations are given as:

$$n(x,t) = n(x) \tag{16}$$

$$p(x,t) = p(x) \tag{17}$$

$$\phi(x,t) = \phi(x) \tag{18}$$

The one dimensional time independent continuity equation for transport of electrons is given by:

`

$$-\frac{1}{e}\frac{\partial j_n(x)}{\partial x} = G_n(x,t) - R_n(x) \tag{19}$$

With,

$$j_n(x) = \frac{e\mu_n n(x)\left(\partial E_{Fn}(x)\right)}{\partial x} \tag{20}$$

$$E_{Fn} = E_c(x) + kTln\left(\frac{n(x)}{N_c(x)}\right) \tag{21}$$

For holes:

$$\frac{1}{e}\frac{\partial j_p(x)}{\partial x} = G_p(x,t) - R_p(x) \tag{22}$$

With,

$$j_p(x) = \frac{e\mu_p p(x)\left(\partial E_{Fp}(x)\right)}{\partial x} \tag{23}$$

$$E_{Fp} = E_v(x) - kTln\left(\frac{p(x)}{N_v(x)}\right) \tag{24}$$

Here,

$j_p(x)$ and $j_n(x)$ are hole and electron currents respectively, E_{Fp} and E_{Fn} are the quasi-Fermi levels of holes and electrons respectively, μ_p and μ_n are hole and electron mobilities respectively, $R_p(x)$ and $R_n(x)$ are recombination rates of holes and electrons respectively, E_c and E_v are conduction and valence band energies respectively and N_c and N_v are effective density of states in conduction and valence bands respectively.

4.1.3 Basic recombination models

Four basic recombination models are included in Afors-Het: conduction band to valence band recombination via radiative band to band recombination(R^{BB}), augur recombination (R^{A}), recombination via defect states located within the bandgaps, known as Shockley-Read-Hall recombination (R^{SRH}) andrecombination due to the dangling bonds (R^{DB}).

The total recombination in DC simulation is given by,

$$R_{n,p}(x) = R^{BB}(x) + R^{A}(x) + R^{SRH}(x) + R^{DB}(x) \tag{25}$$

`

4.2 Energy-Band Diagram Simulation

The following data has been used to simulate the energy-band diagrams [15]:

Parameters	P-type a-Si	Intrinsic a-Si	N-type c-Si
Layer Thickness (nm)	2-12	2-6	3×10^{5}
Electron Affinity (eV)	4	4	4.22
Bandgap (eV)	1.8	1.8	1.12
Donor/Acceptor Doping Density (cm^{-3})	1×10^{17}-1×10^{19}	1×10^{16}	1×10^{13}- 1×10^{17}
Electron Mobility (cm^2/V-s)	25	25	1107
Hole Mobility (cm^2/V-s)	5	5	424.6

Table1: Parameters for simulation in Afors-Het.

The default values of Afors-Het are selected for the remaining parameters (electron and hole velocity: 1×10^{7}cm/s, $N_c = 2.0846\times10^{19}$ cm^{-3}, $N_v = 2.685\times10^{19}$ cm^{-3}, Density = 2.328 g/cm^3). Afors-Het uses standard semiconductor values as default values[1].

Using the above data to define the structure in Afors-Het, a number of energy-band diagrams are simulated by changing the layer thickness and doping density. The layer thickness of P-side is varied from 2 nm to 12 nm, with an increment of 2 nm. Similarly, the thickness of intrinsic layer in between is varied from 2 to 6 nm, with 2 nm increment. Finally the donor doping density of the N-side is varied from 10^{13} to $10^{17}$$cm^{-3}$and acceptor doping density at P-side is varied from 10^{17} to 10^{19} cm^{-3}. All the simulation data is exported to Microsoft Excel for further analysis purpose. Figure 6 is a screenshot of parameter input in Afors-Het to simulate the HIT structure and energy-band diagrams.

`

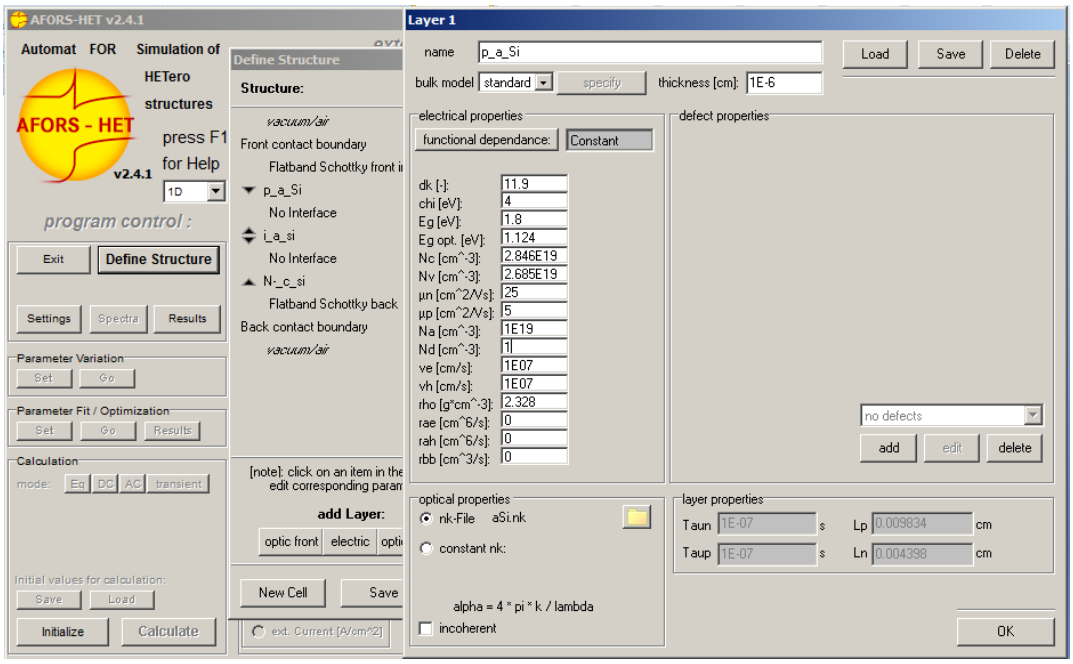

Figure 6: Screenshot of Afors-Het input parameters in structure defining.

An energy-band diagram of HIT structure generated using Afors-Het is shown in Figure 7.

As can be seen in the energy-band diagram, a potential barrier is formed at the valence band. To mention, the energy of hole increases as we go further downward in the energy axis of the energy-band diagram (Figure 7). This barrier forbids the holes which have lower energy than the highest energy in valence band as shown in the Figure 7, to go from one side to the other. Holes cross the barrier in two ways:

1. Thermionic emission, which occurs when holes gain energy and jump over the barrier to the other side.

2. Quantum tunneling, which occurs when holes tunnel through the barrier.

`

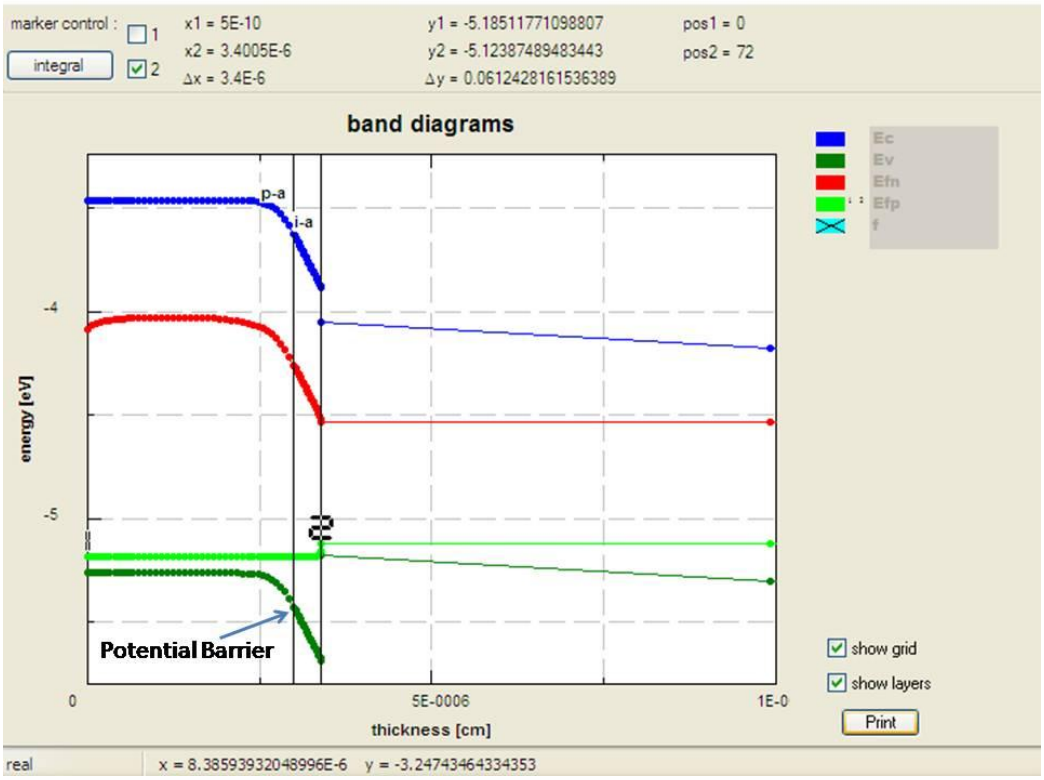

Figure 7: Energy-Band diagram of HIT structure for 5 nm P-type a-Si and 4 nm intrinsic a-Si using Afors-Het

Chapter 5: Transmission Coefficient and Tunneling Current Analysis

The transmission coefficient and tunneling current is calculated in Matlab using the data from the energy-band diagram for each combination of thickness and doping. The transmission coefficient across the potential barrier is calculated usingequation (6). Then, the values of the transmission coefficientsare used to calculate the tunneling current density usingequation (7).

`

It can be seen from (6) that the transmission coefficient is a function of energy (E). The range of energy in valence band from *x1* to *x2* (Figure 8) is divided linearly into 1000 points to obtain 1000 possible energies of holes. *x1* is chosen from the point where the value of the valence band starts to change i.e. where the potential barrier of the valence band starts, and *x2* is chosen where it ends. Value of *x1* for calculating transmission coefficient for each hole energy (E) is the value of the corresponding distance of the barrier energy on which the hole is incident.On the other hand, the value of *x2* remains unchanged due to the shape of the potential barrier.To calculate the transmission coefficient across the potential barrier, we have taken data range starting from the point where the energy of the hole is minimum, to the point just before where it is maximum at the negative end (E_{vmin} in Figure 8).

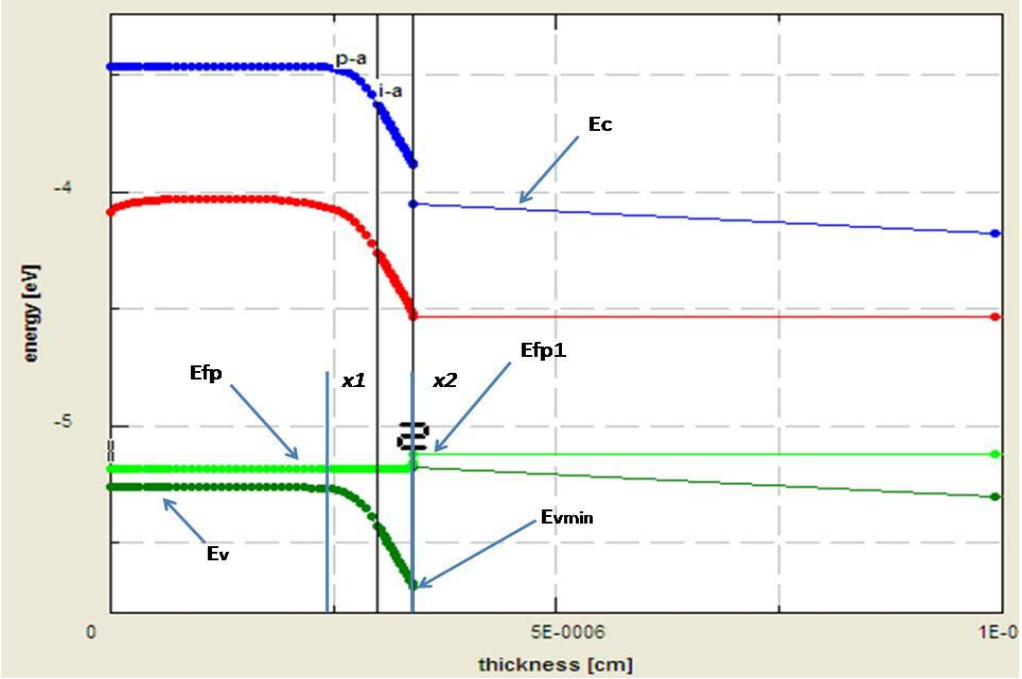

Figure 8: Energy-Band diagram with Evmin, Ev, Ec, Efp and limit of integration x1 and x2 is pointed out.

Figure 9 is the Matlab plot of transmission coefficient versus energy.

`

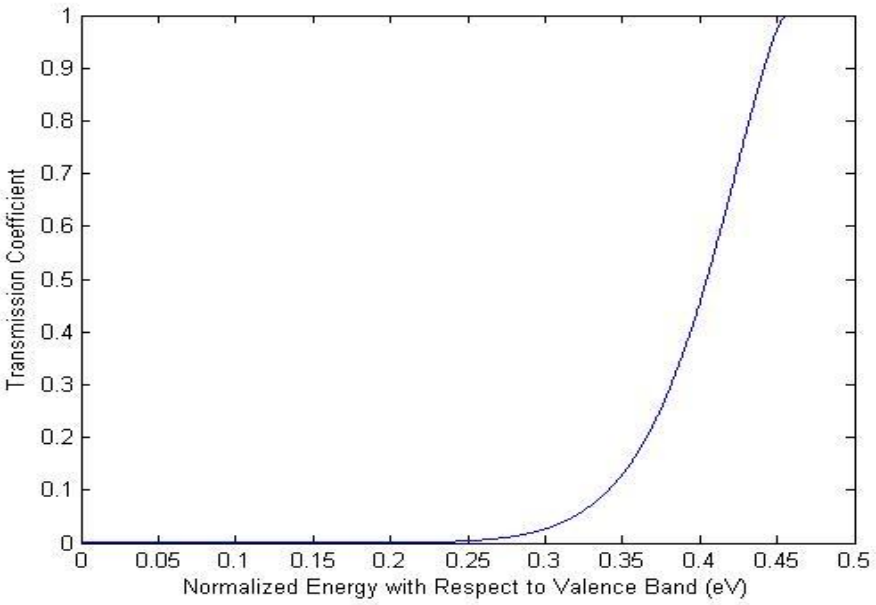

Figure 9: Transmission coefficient for 25 nm p-type a-Si and 2 nm intrinsic a-Si.

In Figure9, a normalized energy with respect to the energy of the valence band is taken for the transmission coefficient plot. As can be seen, the transmission coefficient increases with increase of the hole energy. This is because transmission coefficient is a function of energy, and it increases as the energy of the incident particle increases; which increases the probability of tunneling.

The tunneling current density is not directly calculated using equation (7), discussed in section 3.2 of Chapter 3. As can be seen from the equation, the number of particles (holes in this context)is a function of both position and energy. The number of holes found from the simulation data of Afors-Het is given only as a function of position, not energy. This data indicates that, the total number of holes distributed per unit volume of the valence band is known, but the distribution of holes over energy in a certain volume is not known. In other words, appropriate data to calculate the tunneling current using equation (7) is unavailable from the simulation data.

To overcome the difficulty, a simple assumption has been made to be able to use the available data in equation(7) properly. As the energy of the valence band on the left side of the potential barrier does not vary abruptly, it can be concluded that the change in the number of holes distributed over energy at a certain position is not abrupt. Therefore, the change in the number of holes with changing energy can be considered as a constant.

`

Let, the number of holes at the initial position or position 0 be $p(0)$. From the assumption we can conclude that,

$$p(0) = \int p(0,E)dE = p_{av}(0)\Delta E \tag{26}$$

or $$p_{av}(0) = \frac{p(0)}{\Delta E} \tag{27}$$

The total number of holes per unit volume at position 0, independent of energy is available from the simulation data; and $\Delta E = E_2 - E_1$ .Therefore $p_{av}(0)$ gives the number of holes per unit volume per unit energy at position 0. Similarly we can conclude for the holes on the other side of the barrier, in position R,

$$p(R) = \int p(R,E)dE = p_{av}(R)\Delta E \tag{28}$$

or $$p_{av}(R) = \frac{p(R)}{\Delta E}$$

(29)

Where,

$p_{av}(R)$ is the number of holes perunit volume per unit energy at position R.Hence, we obtain the number of holes as a function of both position and energy.Therefore the equation used to calculate the tunneling current density is given as:

$$J = \frac{e}{2}p_{av}(0)\int_{E_1}^{E_2}|T(E)|^2\ v(0,E)\ dE - \frac{e}{2}\ p_{av}(R)\int_{E_1}^{E_2}|T(E)|^2\ v(R,E)\ dE \tag{30}$$

Here,

$v(0,E)$ and $v(R,E)$ are velocities of holes as a function of energy at position 0 and R respectively.

The limit of integration,E_1 and E_2,in the equation is defined from the starting value or the minimum hole energy in the valence band, to the value where it is maximum.

`

5.1 Effects of Changing Parameters on Tunneling current

Once the algorithm for calculating transmission coefficient and tunneling current has been developed in Matlab, the analysis is done for several combinations of lengths and doping densities. The length of the P-type a-Si and intrinsic a-Si is changed over the range given in Table 1 to determine at which combination of length the value of tunneling current is maximum. After determining the optimum combination, the doping densities of the P-type a-Si and the N-type c-Si is varied and the optimum doping density and the thickness of the p-Si and i-Si to get maximum tunneling current is determined.

5.1.1 Changing Lengths of P-side and Intrinsic Layer

By changing the P-side and intrinsic layer thickness both transmission coefficient and tunneling current is calculated. Simulations of transmission coefficients for changing the P-side from 2 nm to 12 nm and plotting the data give the following curves:

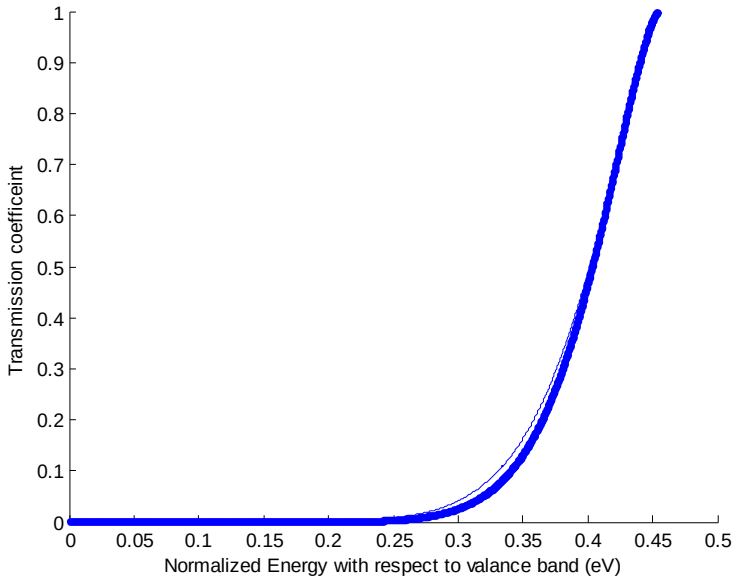

Figure 10: Transmission coefficients for changing lengths of P-side from 2nm to 12 nm, with 4 nm intrinsic thickness.

As can be seen from the curve, despite of having 6 plots (for all the changing lengths of P-side) for the values of transmission coefficients, no major changes can be noticed. The effect of change in the transmission coefficient can be seen in Figure 10. As can be seen from the plot in

`

Figure 11, the tunneling current density is above 4×10^{10}A/m^{2}for P-side length 3-12 nm. It decreases to below 3.8×10^{10}A/m^{2}at 12 nm P-side length. The plot of the tunneling current densities versus lengths of P-side is shown in Figure 11.

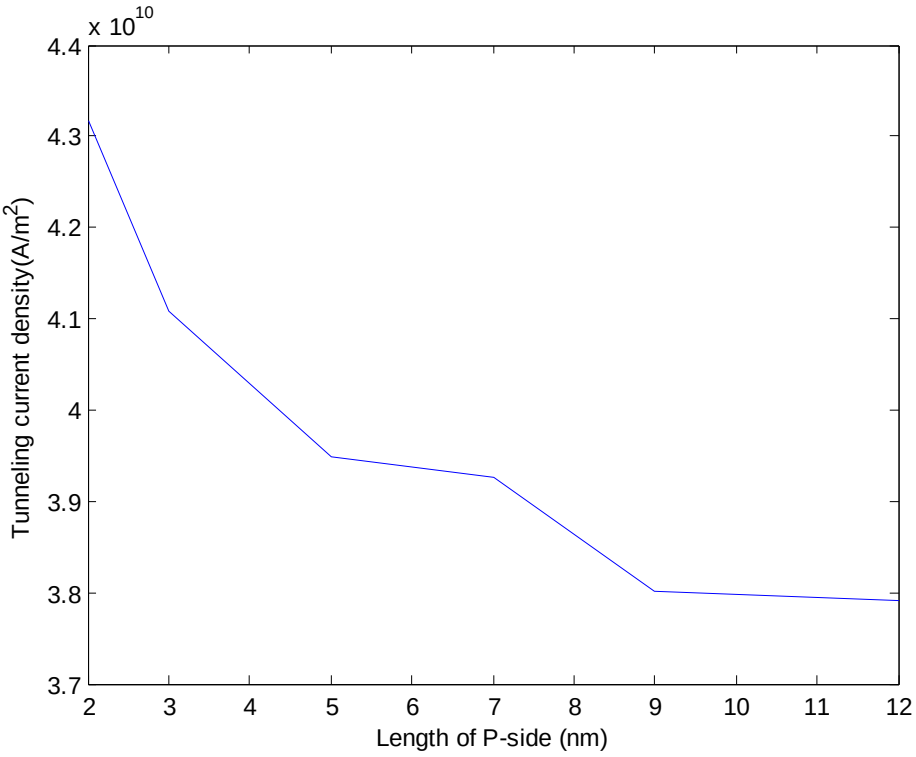

Figure 11: Tunneling current density with changing lengths of P-side, with 4 nm intrinsic layer thickness.

Although the current density at 2 nm is slightly more than the current density at 5 nm, it is preferable to choose 5 nm P-side length, considering the decrease in the J_{sc} and the fill factor. There is also the overall degradation of cell device [15].

Therefore, considering the circumstances, optimized length of P-side is 5 nm.

Changing the intrinsic layer thickness, on the other hand has effect on the transmission coefficient and tunneling current. The intrinsic layer thickness is varied from 2 nm to 6 nm. The plots of the transmission coefficients for each thickness of the intrinsic layer are shown below in Figure12.

`

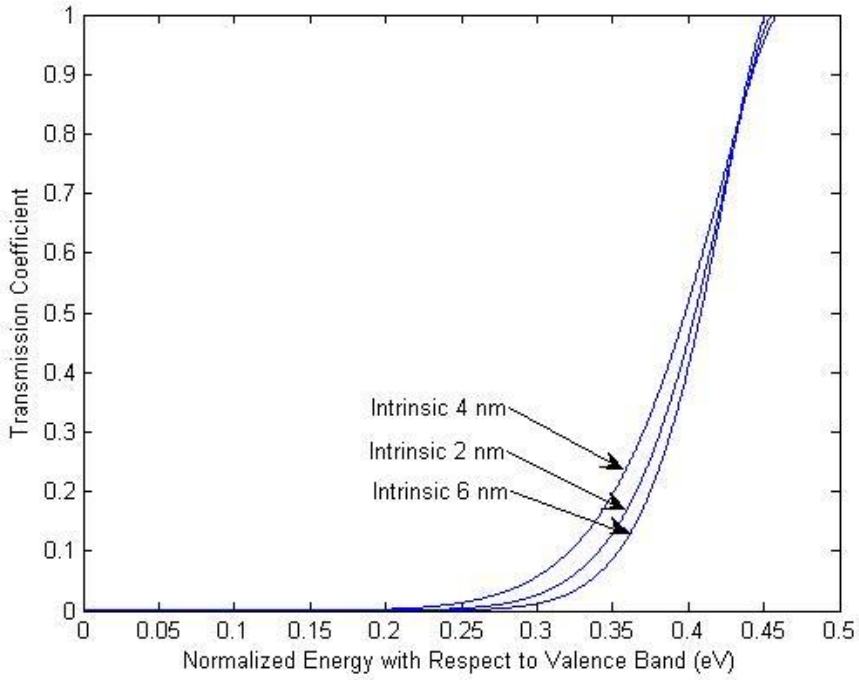

Figure 12: Transmission coefficient with changing intrinsic layer thickness from 2 nm to 6 nm, with 5 nm P-sidethickness.

Such change in the transmission coefficient has measurable impact on tunneling process. Tunneling current density for each thickness of the intrinsic layer is shown in the plot below in Figure13.

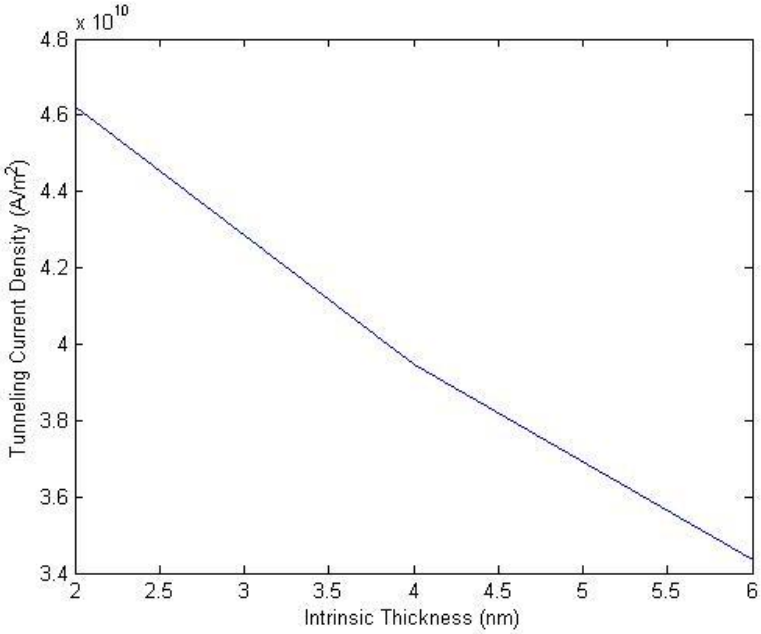

Figure 13: Tunneling current density with changing lengths of intrinsic layer, with 5 nm P-side thickness.

`

As can be seen from Figure 13, the value of the tunneling current density isthe highest for 2 nm intrinsic thickness. It is calculated that the value of tunneling current decreases with increase in the thickness of the intrinsic layer. But due to the difficulty in fabrication process of 2nm, and it also decreases the fill factor [15], 4 nm intrinsic layer is considered as optimum thickness for intrinsic layer.

Therefore, the optimum thickness of the intrinsic layer is 4 nm.

5.1.2 Changing Doping Densities of P and N sides

The doping densities of both P-type a-Si and N-type c-Si have strong impacts on the tunneling process. Increasing the doping density in the P-side from 10^{17} cm^3 to 10^{19} cm^3 has a significant impact on the transmission coefficient. The plots of the transmission coefficient for each acceptor doping density are shown Figure 14.

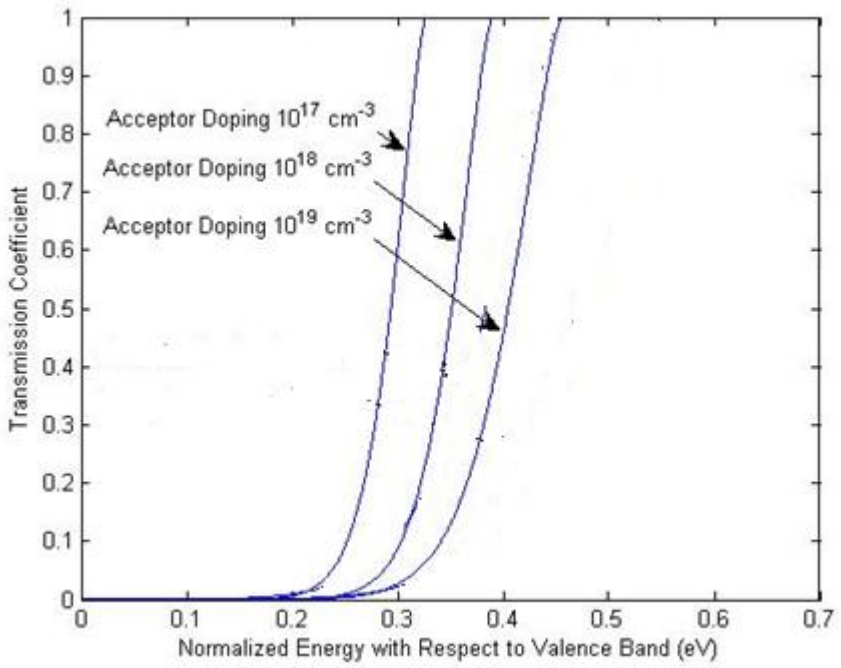

Figure 14: Transmission coefficient for each acceptor doping density of the P-side.

As can be seen from the simulation data from Afors-Het, the height of the barrierincreases as the doping density increases. Consequently, the transmission coefficient shifts to the right, as can be seen in Figure 14.This change in the transmission coefficienthas measurable impact on the tunneling current. Increasing doping density increases the tunneling current density as shown in Figure 15.

`

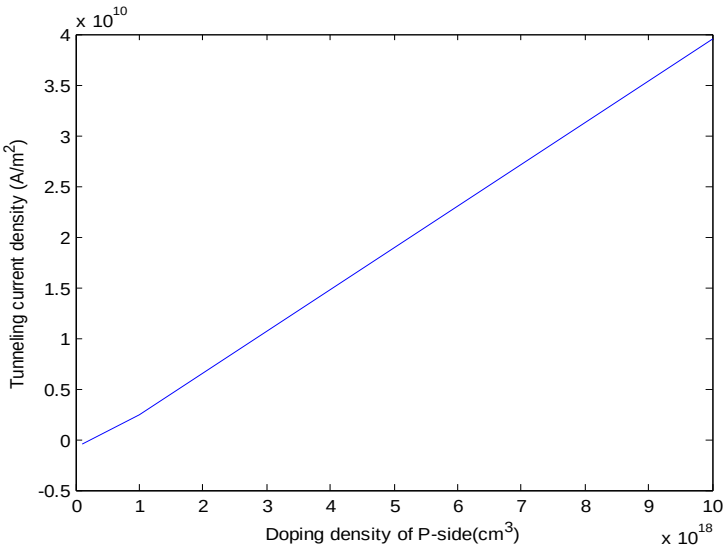

Figure 15: Tunneling current density for increasing acceptor doping density at P-side.

Therefore, the optimum acceptor doping density for p-side is 10^{19} cm^{-3}.

Increasing the doping density in the c-Si decreases the tunneling current significantly. The donor doping density of the c-Si has been changed from 10^{13} cm^{-3} to 10^{17} cm^{-3} to simulate the transmission coefficients and the tunneling currents. Figure-16 shows the transmission coefficients for each doping density:

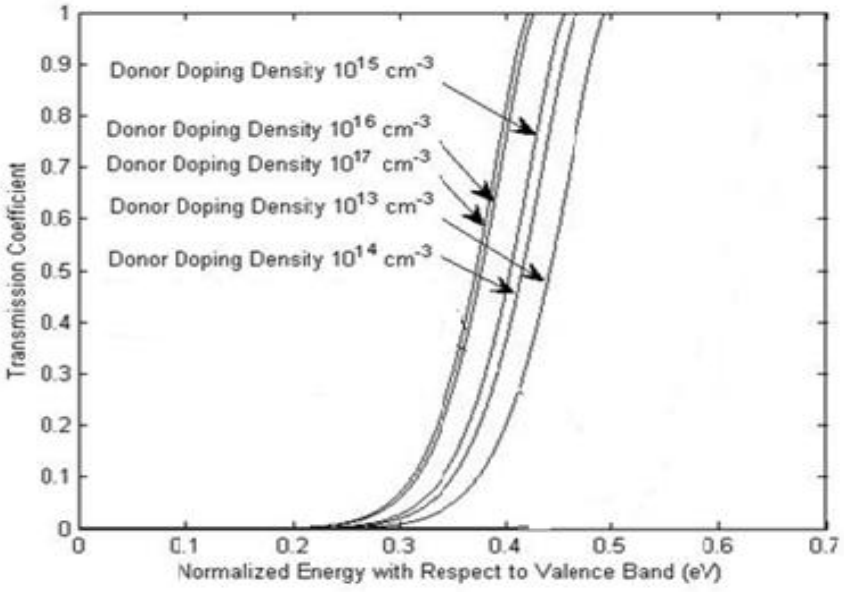

Figure 16: Transmission coefficient for each donor doping density of the N-side.

`

As it can be seen from the curves, the transmission coefficients show significant change with changing doping density. This change in the transmission coefficient has measurable impact on the tunneling current. Increasing doping density decreases the tunneling current density as can be seen from plot of the tunneling current densities with each doping density in Figure 17.

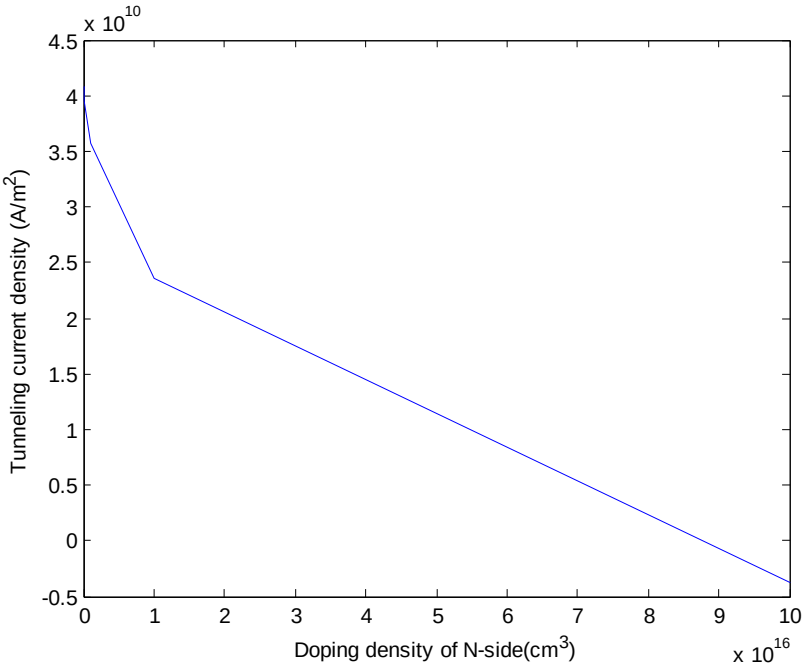

Figure 17: Tunneling current density for increasing donor doping density at N-side.

The current density is maximum at low doping (10^{13} cm^{-3}) and decreases as the doping density increases. Therefore, it can be concluded that the lower the donor doping at the N-side, the more tunneling of holes, and more tunneling current.

Therefore, the optimum donor doping density for N-side is 10^{13} cm^{-3}.

`

Chapter 6: Summary

In this document, the tunneling current of a HIT structure has been analyzed. Due to the difference of bandgap in heterojunctions, a potential barrier at the valence band (for N-type HIT) or the conduction band (P-type HIT) forms. This reduces the overall current of the device. However, the holes and electrons can tunnel through the potential barrier (quantum mechanical tunneling) and create a small current which adds to the overall current. An increase in the tunneling current increases the overall current. To have a maximum tunneling current, the length and doping parameters have been considered and analyzed to propose an optimized structure of HIT.

6.1 Conclusion

The length of the P-side of the HIT structure has been varied from 2 nm to 12 nm to determine which configuration gives the most current. As seen from the simulations, the increase in the length of the P-type a-Si decreases the current. Therefore, the highest value of tunneling current at thickness 5 nm is considered as the optimum thickness of P-side of the HIT structure. Then, the thickness of the intrinsic layer has been varied from 2 nm to 6 nm. It can be seen that at 2 nm thickness tunneling current is maximum, but increasing the thickness of the intrinsic region further, reduces the current density. Therefore, 4 nm intrinsic thickness is concluded as the optimum intrinsic thickness.

Then, the donor doping density of the N-side is varied from 10^{13} cm^{-3} to 10^{17} cm^{-3}. It can be seen that maximum tunneling occurs when the doping density is lowest. Therefore, keeping a low doping density of 10^{13} cm^{-3} at N-side c-Si gives higher tunneling current. On the other hand, the acceptor doping density at the P-type a-Si side is varied from 10^{17} cm^{-3} to 10^{19} cm^{-3}. The tunneling current is seen to increase as doping density increases. Therefore 10^{19} cm^{-3} is the optimum doping density at the P-side a-Si, which gives maximum tunneling current.

6.2 Future Scope of Work

This document is only limited to analysis of a number of parameters in a simple HIT structure. Further scope of work may involve more complex issues and algorithms. A few proposed ways for good scope of working are:

`

a. The structure for which analysis has been done is the simplest form of HIT structure, with only an a-Si P-side, a-Si thin intrinsic layer and a c-Si N-side. Similar analysis can be performed in a more complex structure with multiple junctions and layers.
b. This study is only limited to tunneling current analysis. Efficiency and thermionic emission analysis has not been included, although such analysis is crucial for determining an optimum structure.
c. This document does not analyze the multi-tunneling phenomenon that occurs due to defect states and charge trapping within the band gaps. Multi-tunneling is another important form of charge transport in heterojunctions.
d. A detailed study of the same with more concentration on defect density can be performed for more accurate analysis.

References

`

1. W.G.J.H.M. van Sark, L. Korte and F. Roca, *Physics and Technology of Amorphous-Crystalline Heterostructure Silicon Solar Cells*, Berlin, Germany, Woodhead,2012.

2. D.M Chapin, C.S. Fuller, G.L. Pearson, "A new silicon *p-n* junction photocell for converting solar radiation into electrical power",*J. Appl. Phys*., vol. 25, pp. 676–677, Jan. 1954.

3. M. Tanaka, M. Taguchi, T. Matsuyama, T. Sawada, S. Tsuda, S. Nakano, H. Hanafusa, Y. Kuwano, "Development of new a-Si/c-Si heterojunction solar cells: ACJHIT (artificially constructed junction-heterojunction with Intrinsic thin-layer)", *J. Appl. Phys*., vol. 31, pp. 3518, Sep. 1992.

4. T. Mishima, M. Taguchi, H. Sakata, E. Maruyama, "Development Status of High EfficiencyHIT Solar Cells",*Sol. Energ. Mat. Sol*., vol. 95, no. 18,Apr. 2010.

5. A. Kanevce, W. Metzger, "The Role of Amorphous Silicon and Tunneling in Heterojunction with Intrinsic Thin Layer (HIT) Solar Cells", *J. Appl. Phys*.,vol. 105, no. 094507,May 2009.

6. J. Verschraegen , M. Burgelman, "Numerical Modeling of Intra-Band Tunneling for Heterojunction Solar Cells in SCAPS", *Thin Sol. Film.*,vol. 515,pp. 6276–6279, Jan. 2007.

7. K. Yang, J. R. East and G. I. Haddad, "Numerical Modeling of Abrupt Heterojunctions using a Thermionic-Field Emission Boundary Condition",*Sol. Stat. Electron*.,vol. 36, no. 3, pp. 321-330, 1993.

`

8. M. Ferrara, "Electroluminescence of a-Si/c-Si Heterojunction Solar Cells after High Energy Irradiation", Ph.D dissertation, Dept. of Mathematics and Computer Science, The Open University in Hagen, Hegan, Germany, 2002.

9. T. F. Schulze, Structural, "Electronic and Transport Properties of Amorphous/Crystalline Silicon Heterojunctions", Ph.D. dissertation, Dept. of Mathematics and Science, Berlin University of Technology, Berlin, Germany, 2011.

10. J. Appenzeller, M. Radosavljevic´, J. Knoch, P. Avouris, "TunnelingVersus Thermionic Emission in One-Dimensional Semiconductors", *Phys. Rev. Lett*., vol. 92, no. 4, pp 8301-1, Jan. 2004.

11. S. M. Sze, K. K. Ng, *Physics of Semiconductor Devices*, Third Edition, New Delhi, India, Wiley-Interscience, 2007.

12. R. L. Anderson,"Ge-GaAs Heterojunctions",*IBM J. Res. Dev.*,vol. 4, no. 3, pp. 283-287, 1960.

13. R. Tsu and L. Esaki,"Tunneling in a Finite Superlattice", *Appl. Phys. Lett.*, vol. 22, no. 11, pp-562, Jun. 1973.

14. R. Stangl, C. Leendertz, J. Haschke (2010), *Numerical Simulation of Solar Cells and Solar Cell Characterization Methods: the Open-Source on Demand Program Afors-Het*,in *SolarEnergy*, [online], available at: http://www.intechopen.com/books/solar-energy/numerical-simulation-of-solar-cells-and-solar-cell-characterization-methods-the-open-source-on-deman

15. A. Datta and P. Chatterjee,"Computer Modeling of Heterojunction with Intrinsic Thin Layer "HIT" Solar Cells: Sensitivity Issues and Insights Gained", in *Solar Cells - Thin-Film Technologies*,First edition,Rijeka, Croatia,InTech, 2011, Chapter 13, pp. 282.

`